

Proceedings of the 12th International Conference on
Computational Fluid Dynamics in the Oil & Gas,
Metallurgical and Process Industries

Progress in Applied CFD – CFD2017



SINTEF Proceedings

Editors:

Jan Erik Olsen and Stein Tore Johansen

Progress in Applied CFD – CFD2017

Proceedings of the 12th International Conference on Computational Fluid Dynamics
in the Oil & Gas, Metallurgical and Process Industries

SINTEF Academic Press

SINTEF Proceedings no 2

Editors: Jan Erik Olsen and Stein Tore Johansen

Progress in Applied CFD – CFD2017

Selected papers from 10th International Conference on Computational Fluid Dynamics in the Oil & Gas, Metallurgical and Process Industries

Key words:

CFD, Flow, Modelling

Cover, illustration: Arun Kamath

ISSN 2387-4295 (online)

ISBN 978-82-536-1544-8 (pdf)

© Copyright SINTEF Academic Press 2017

The material in this publication is covered by the provisions of the Norwegian Copyright Act. Without any special agreement with SINTEF Academic Press, any copying and making available of the material is only allowed to the extent that this is permitted by law or allowed through an agreement with Kopinor, the Reproduction Rights Organisation for Norway. Any use contrary to legislation or an agreement may lead to a liability for damages and confiscation, and may be punished by fines or imprisonment

SINTEF Academic Press

Address: Forskningsveien 3 B
 PO Box 124 Blindern
 N-0314 OSLO

Tel: +47 73 59 30 00

Fax: +47 22 96 55 08

www.sintef.no/byggforsk

www.sintefbok.no

SINTEF Proceedings

SINTEF Proceedings is a serial publication for peer-reviewed conference proceedings on a variety of scientific topics.

The processes of peer-reviewing of papers published in SINTEF Proceedings are administered by the conference organizers and proceedings editors. Detailed procedures will vary according to custom and practice in each scientific community.

PREFACE

This book contains all manuscripts approved by the reviewers and the organizing committee of the 12th International Conference on Computational Fluid Dynamics in the Oil & Gas, Metallurgical and Process Industries. The conference was hosted by SINTEF in Trondheim in May/June 2017 and is also known as CFD2017 for short. The conference series was initiated by CSIRO and Phil Schwarz in 1997. So far the conference has been alternating between CSIRO in Melbourne and SINTEF in Trondheim. The conferences focuses on the application of CFD in the oil and gas industries, metal production, mineral processing, power generation, chemicals and other process industries. In addition pragmatic modelling concepts and bio-mechanical applications have become an important part of the conference. The papers in this book demonstrate the current progress in applied CFD.

The conference papers undergo a review process involving two experts. Only papers accepted by the reviewers are included in the proceedings. 108 contributions were presented at the conference together with six keynote presentations. A majority of these contributions are presented by their manuscript in this collection (a few were granted to present without an accompanying manuscript).

The organizing committee would like to thank everyone who has helped with review of manuscripts, all those who helped to promote the conference and all authors who have submitted scientific contributions. We are also grateful for the support from the conference sponsors: ANSYS, SFI Metal Production and NanoSim.

Stein Tore Johansen & Jan Erik Olsen



Organizing committee:

Conference chairman: Prof. Stein Tore Johansen

Conference coordinator: Dr. Jan Erik Olsen

Dr. Bernhard Müller

Dr. Sigrid Karstad Dahl

Dr. Shahriar Amini

Dr. Ernst Meese

Dr. Josip Zoric

Dr. Jannike Solsvik

Dr. Peter Witt

Scientific committee:

Stein Tore Johansen, SINTEF/NTNU

Bernhard Müller, NTNU

Phil Schwarz, CSIRO

Akio Tomiyama, Kobe University

Hans Kuipers, Eindhoven University of Technology

Jinghai Li, Chinese Academy of Science

Markus Braun, Ansys

Simon Lo, CD-adapco

Patrick Segers, Universiteit Gent

Jiyuan Tu, RMIT

Jos Derksen, University of Aberdeen

Dmitry Eskin, Schlumberger-Doll Research

Pär Jönsson, KTH

Stefan Pirker, Johannes Kepler University

Josip Zoric, SINTEF

CONTENTS

PRAGMATIC MODELLING	9
On pragmatism in industrial modeling. Part III: Application to operational drilling	11
CFD modeling of dynamic emulsion stability	23
Modelling of interaction between turbines and terrain wakes using pragmatic approach	29
FLUIDIZED BED	37
Simulation of chemical looping combustion process in a double looping fluidized bed reactor with cu-based oxygen carriers.....	39
Extremely fast simulations of heat transfer in fluidized beds.....	47
Mass transfer phenomena in fluidized beds with horizontally immersed membranes	53
A Two-Fluid model study of hydrogen production via water gas shift in fluidized bed membrane reactors	63
Effect of lift force on dense gas-fluidized beds of non-spherical particles	71
Experimental and numerical investigation of a bubbling dense gas-solid fluidized bed	81
Direct numerical simulation of the effective drag in gas-liquid-solid systems	89
A Lagrangian-Eulerian hybrid model for the simulation of direct reduction of iron ore in fluidized beds.....	97
High temperature fluidization - influence of inter-particle forces on fluidization behavior	107
Verification of filtered two fluid models for reactive gas-solid flows	115
BIOMECHANICS.....	123
A computational framework involving CFD and data mining tools for analyzing disease in carotid artery	125
Investigating the numerical parameter space for a stenosed patient-specific internal carotid artery model.....	133
Velocity profiles in a 2D model of the left ventricular outflow tract, pathological case study using PIV and CFD modeling.....	139
Oscillatory flow and mass transport in a coronary artery.....	147
Patient specific numerical simulation of flow in the human upper airways for assessing the effect of nasal surgery.....	153
CFD simulations of turbulent flow in the human upper airways	163
OIL & GAS APPLICATIONS	169
Estimation of flow rates and parameters in two-phase stratified and slug flow by an ensemble Kalman filter	171
Direct numerical simulation of proppant transport in a narrow channel for hydraulic fracturing application	179
Multiphase direct numerical simulations (DNS) of oil-water flows through homogeneous porous rocks	185
CFD erosion modelling of blind tees	191
Shape factors inclusion in a one-dimensional, transient two-fluid model for stratified and slug flow simulations in pipes	201
Gas-liquid two-phase flow behavior in terrain-inclined pipelines for wet natural gas transportation	207

NUMERICS, METHODS & CODE DEVELOPMENT	213
Innovative computing for industrially-relevant multiphase flows	215
Development of GPU parallel multiphase flow solver for turbulent slurry flows in cyclone.....	223
Immersed boundary method for the compressible Navier–Stokes equations using high order summation-by-parts difference operators	233
Direct numerical simulation of coupled heat and mass transfer in fluid-solid systems	243
A simulation concept for generic simulation of multi-material flow, using staggered Cartesian grids.....	253
A cartesian cut-cell method, based on formal volume averaging of mass, momentum equations.....	265
SOFT: a framework for semantic interoperability of scientific software	273
 POPULATION BALANCE	 279
Combined multifluid-population balance method for polydisperse multiphase flows	281
A multifluid-PBE model for a slurry bubble column with bubble size dependent velocity, weight fractions and temperature.....	285
CFD simulation of the droplet size distribution of liquid-liquid emulsions in stirred tank reactors	295
Towards a CFD model for boiling flows: validation of QMOM predictions with TOPFLOW experiments	301
Numerical simulations of turbulent liquid-liquid dispersions with quadrature-based moment methods.....	309
Simulation of dispersion of immiscible fluids in a turbulent couette flow	317
Simulation of gas-liquid flows in separators - a Lagrangian approach.....	325
CFD modelling to predict mass transfer in pulsed sieve plate extraction columns	335
 BREAKUP & COALESCENCE	 343
Experimental and numerical study on single droplet breakage in turbulent flow	345
Improved collision modelling for liquid metal droplets in a copper slag cleaning process	355
Modelling of bubble dynamics in slag during its hot stage engineering.....	365
Controlled coalescence with local front reconstruction method	373
 BUBBLY FLOWS	 381
Modelling of fluid dynamics, mass transfer and chemical reaction in bubbly flows	383
Stochastic DSMC model for large scale dense bubbly flows.....	391
On the surfacing mechanism of bubble plumes from subsea gas release.....	399
Bubble generated turbulence in two fluid simulation of bubbly flow	405
 HEAT TRANSFER	 413
CFD-simulation of boiling in a heated pipe including flow pattern transitions using a multi-field concept	415
The pear-shaped fate of an ice melting front	423
Flow dynamics studies for flexible operation of continuous casters (flow flex cc).....	431
An Euler-Euler model for gas-liquid flows in a coil wound heat exchanger.....	441
 NON-NEWTONIAN FLOWS.....	 449
Viscoelastic flow simulations in disordered porous media	451
Tire rubber extrudate swell simulation and verification with experiments	459
Front-tracking simulations of bubbles rising in non-Newtonian fluids.....	469
A 2D sediment bed morphodynamics model for turbulent, non-Newtonian, particle-loaded flows.....	479

METALLURGICAL APPLICATIONS.....	491
Experimental modelling of metallurgical processes	493
State of the art: macroscopic modelling approaches for the description of multiphysics phenomena within the electroslag remelting process	499
LES-VOF simulation of turbulent interfacial flow in the continuous casting mold	507
CFD-DEM modelling of blast furnace tapping	515
Multiphase flow modelling of furnace tapholes	521
Numerical predictions of the shape and size of the raceway zone in a blast furnace.....	531
Modelling and measurements in the aluminium industry - Where are the obstacles?	541
Modelling of chemical reactions in metallurgical processes.....	549
Using CFD analysis to optimise top submerged lance furnace geometries	555
Numerical analysis of the temperature distribution in a martensitic stainless steel strip during hardening.....	565
Validation of a rapid slag viscosity measurement by CFD.....	575
Solidification modeling with user defined function in ANSYS Fluent.....	583
Cleaning of polycyclic aromatic hydrocarbons (PAH) obtained from ferroalloys plant.....	587
Granular flow described by fictitious fluids: a suitable methodology for process simulations	593
A multiscale numerical approach of the dripping slag in the coke bed zone of a pilot scale Si-Mn furnace.....	599
INDUSTRIAL APPLICATIONS	605
Use of CFD as a design tool for a phosphoric acid plant cooling pond	607
Numerical evaluation of co-firing solid recovered fuel with petroleum coke in a cement rotary kiln: Influence of fuel moisture	613
Experimental and CFD investigation of fractal distributor on a novel plate and frame ion-exchanger	621
COMBUSTION	631
CFD modeling of a commercial-size circle-draft biomass gasifier.....	633
Numerical study of coal particle gasification up to Reynolds numbers of 1000.....	641
Modelling combustion of pulverized coal and alternative carbon materials in the blast furnace raceway	647
Combustion chamber scaling for energy recovery from furnace process gas: waste to value	657
PACKED BED.....	665
Comparison of particle-resolved direct numerical simulation and 1D modelling of catalytic reactions in a packed bed	667
Numerical investigation of particle types influence on packed bed adsorber behaviour	675
CFD based study of dense medium drum separation processes	683
A multi-domain 1D particle-reactor model for packed bed reactor applications.....	689
SPECIES TRANSPORT & INTERFACES	699
Modelling and numerical simulation of surface active species transport - reaction in welding processes	701
Multiscale approach to fully resolved boundary layers using adaptive grids.....	709
Implementation, demonstration and validation of a user-defined wall function for direct precipitation fouling in Ansys Fluent.....	717

FREE SURFACE FLOW & WAVES	727
Unresolved CFD-DEM in environmental engineering: submarine slope stability and other applications.....	729
Influence of the upstream cylinder and wave breaking point on the breaking wave forces on the downstream cylinder	735
Recent developments for the computation of the necessary submergence of pump intakes with free surfaces	743
Parallel multiphase flow software for solving the Navier-Stokes equations	752
 PARTICLE METHODS	 759
A numerical approach to model aggregate restructuring in shear flow using DEM in Lattice-Boltzmann simulations	761
Adaptive coarse-graining for large-scale DEM simulations.....	773
Novel efficient hybrid-DEM collision integration scheme.....	779
Implementing the kinetic theory of granular flows into the Lagrangian dense discrete phase model.....	785
Importance of the different fluid forces on particle dispersion in fluid phase resonance mixers	791
Large scale modelling of bubble formation and growth in a supersaturated liquid.....	798
 FUNDAMENTAL FLUID DYNAMICS	 807
Flow past a yawed cylinder of finite length using a fictitious domain method	809
A numerical evaluation of the effect of the electro-magnetic force on bubble flow in aluminium smelting process.....	819
A DNS study of droplet spreading and penetration on a porous medium.....	825
From linear to nonlinear: Transient growth in confined magnetohydrodynamic flows.....	831

NOVEL EFFICIENT HYBRID-DEM COLLISION INTEGRATION SCHEME

Kay A. BUIST^{1*}, Luuk J.H. SEELEN¹, Niels G. DEEN², Johan T. PADDING³, Hans J.A.M. KUIPERS¹

¹Multiphase Reactors group, Department of Chemical Engineering & Chemistry, Eindhoven University of Technology, P.O. box 513, 5600 MB Eindhoven, The Netherlands

²Multiphase & Reactive Flows Group, Department of Mechanical Engineering, Eindhoven University of Technology, P.O. Box 513, 5600 MB Eindhoven, The Netherlands

³Intensified Reaction and Separation Systems Group, Process & Energy department, Delft University of Technology, Leeghwaterstraat 39, 2628 CA Delft, The Netherlands

* E-mail: k.a.buist@tue.nl

ABSTRACT

A hybrid collision integration scheme is introduced, benefiting from the efficient handling of binary collisions in the hard sphere scheme and the robust time scaling of the soft sphere scheme. In typical dynamic dense granular flow, simulated with the soft sphere scheme, the amount of collisions involving more than two particles are limited, and necessarily so because of loss of energy decay otherwise. Because most collisions are binary, these collisions can be handled within one time step without the necessary numerical integration as needed in a soft sphere method. The remainder of the collisions can still be handled with the classical soft sphere scheme. In this work the hybrid collisions integration scheme is shortly described and tested with a bounding box problem. The hybrid scheme is capable of solving the same problem as a classic soft sphere scheme but is roughly one order of magnitude faster.

Keywords: Discrete Element Method, Collision integration scheme, optimization .

p position, [m].
 d diameter, [m].
 c integration constant, [-].

Sub/superscripts

0 old time step
 n normal
 d dampened
 t tangential
 $coll$ collision
 a, b particles a, b
 $last$ duration of lasting collision
 i index i
 max maximum
 s solids
 eff effective

NOMENCLATURE

Greek Symbols

δ overlap, [m]
 ω frequency, [1/s]
 ζ damping ratio, [-]
 η damping coefficient, [Ns/m]
 μ friction coefficient, [-]
 β tangential restitution coefficient, [kg/m³]
 ρ density, [kg/m³]
 ϕ solids volume fraction, [-]

Latin Symbols

\vec{F} force, [kgm/s²].
 \vec{J} impuls, [kgm/s].
 B collision constant, [kg⁻¹].
 R norm of distance, [m].
 N number of particles, [-].
 \vec{v} velocity, [m/s].
 t time, [s].
 m mass, [kg].
 k spring stiffness, [N/m].
 \vec{n} normal unit vector, [-].
 e restitution coefficient, [-].
 f frequency, [1/s].
 \vec{x} position vector, [m].
 \vec{r} distance vector, [m].

INTRODUCTION

Since the introduction of the Distinct Element Model (DEM) by Cundall and Strack (1979) for perfect spheres the field of granular flow modelling has expanded dramatically. The model by Cundall and Strack (1979) has since then been extended for various external forces (Xu and Yu, 1997; Pournin *et al.*, 2005; Lu *et al.*, 2015; Marshall, 2009; Mikami *et al.*, 1998; Korevaar *et al.*, 2014; Zastawny *et al.*, 2012). For an overview of the relevant inter-particle and particle-fluid forces see Zhu *et al.* (2007). DEM has been used to model various granular flows as found in industrial applications, ranging from; fluidized beds (Van Buijtenen *et al.*, 2011), rotating drums (Gonzalez Briones *et al.*, 2015; Yang *et al.*, 2008) and tumbling mills, chute flow (Shirsath *et al.*, 2014) to sedimentation and hoppers (Cleary and Sawley, 2002). A more comprehensive overview of these applications can be found in the work of Zhu *et al.* (2008).

The foundation of these models is however the contact model, of which the hard sphere model as discussed by Hoomans *et al.* (1996) and a soft sphere model by Tsuji *et al.* (1993) are the most well known. The hard-sphere approach works on the assumption that all collisions are binary and instantaneous. As such the model only handles particle-pair interactions that follow each other in chronological order. Therefore the hard-sphere model is an event-driven scheme and the simulation time scales with the collision frequency, which scales with the solids fraction and the granular temperature of the system. The hard-sphere scheme is most suited for rather dilute systems, as with increasing solids fraction

and granular temperature the number of collisions increases drastically.

For more dense and highly dynamic systems a soft-sphere method is more often used. The soft-sphere method allows for particle-particle overlap and represents the forces associated with the indentation of the solids with a spring-dashpot system. The spring handles the repulsion and the dashpot handles energy dissipation. The duration of the collision is no longer instantaneous and scales with the ratio of the spring stiffness and the mass of the particle. Because of the finite duration of the collision multiple particles can be in contact at the same time, in this work denoted as Multi-Body Collisions (MBC). Numerical integration of the forces over time allows for proper treatment of the collisions. The soft-sphere method is thus a time-driven scheme.

Both methodologies have their strengths and limitations. The hard-sphere model benefits from the immediate handling of a collision, while the soft-sphere method benefits from the relaxation of the spring-stiffness and thus larger time step. The most time-consuming step in the simulations however is the collision detection, which for the hard-sphere has to be updated with a frequency related to the number of events and for the soft-sphere has to be performed every particle time step; roughly ten times per duration of the collision. Reducing the number of collision detection evaluations thus massively increases the simulation efficiency.

In the soft-sphere method, for dynamical systems, most of the collisions will still be binary. And they have to be mostly binary, because else the energy dissipation rate is no longer maintained, as we will show later. In one of our simulations from earlier work (Buist *et al.* (2015)) we indeed found that most collisions involved only two particles, as can be seen in figure 1.

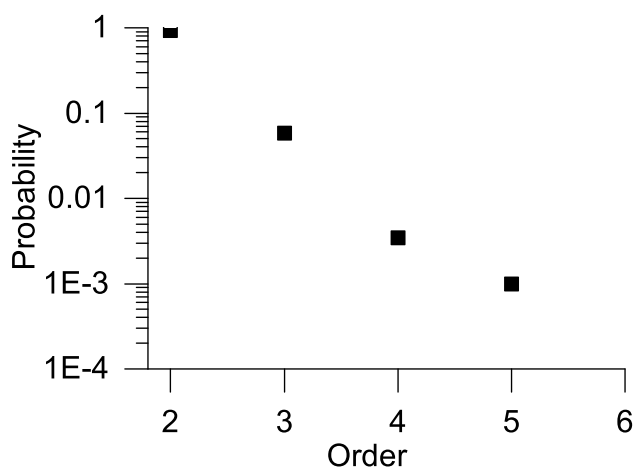


Figure 1: Collision order probability from a simulation of a pseudo 2D fluidized bed, with $\varepsilon = 0 - 0.6$, $u_{mf} = 3.5$ m/s, $e = 1$, $\beta = 0.33$, $\mu = 0.1$.

All of these binary collisions can of course be handled instantaneously, following the analytical solution of the damped harmonic oscillator. The binary collision maintains a finite duration and the task that remains is to be able to distinguish between binary collisions and Multi-Body contacts. These MBC's have to be solved with a classical soft-sphere method. The collisions have to be determined only once, and only for the particles colliding in two subsequent time steps additional checks have to be made. The time-step of the simulation is now exactly the duration of a collision, and collision-detection has to be performed only once for most

of the particles. This work is a short version of a publication in Chemical Engineering Science, containing the main idea of the hybrid collision integration scheme and the main results. For more details the interested reader is referred to Buist *et al.* (2016).

MODEL DESCRIPTION

The hybrid model is in spirit somewhere in between a hard sphere and a soft sphere methodology. In this work however we will not go into the details of these two methods, for an extensive explanation of both schemes the interested reader is referred to Deen *et al.* (2007).

Hybrid DEM

The new integration scheme can either be viewed as a time-driven hard sphere model with a finite collision duration or as a semi one-step soft sphere model. A time-driven hard sphere approach was first developed by Helland *et al.* (2002). In their work however, each collision is still quasi-instantaneous. The first to couple a hard sphere and a soft sphere approach was Gui *et al.* (2016). In their work however the time step used is still considerably smaller than the duration of a collision. The use of a hard sphere methodology however allows for an accurate description of collisions, while maintaining a ~ 10 times larger time step with respect to a classical visco-elastic methodology for non-spherical particles.

In the hybrid collision integration scheme that is presented here, the chosen time step is exactly the same as the duration of a collision, following the linear spring dashpot model. Because most collisions are assumed to be binary these collisions can be handled at once, following a modified hard sphere approach. And because the time step is the same as the collision duration, only one collision per particle per time step can happen. The only exceptions are the multi-body collisions, that are handled with the classical soft sphere methodology. For the particles involved in a multi-body collision, the time step is divided in ten sub steps. A short schematic overview is given in table 1.

The gain in speed-up is in the use of the collision detection algorithm, which generally has to take place only once every time step, instead of ten times in the classical soft-sphere scheme. Of course the actual choice of the type of collision detection algorithm will have a major impact on the final performance of the codes. In this work the same collision detection algorithm is used for both the classical soft-sphere method and the hybrid method; a kd-tree algorithm from Matlab.

In the next few sections we will discuss in a bit more detail binary collisions and multi-body collisions. Finally an overview of the model is given that shows the main extra steps that need to be taken into account.

Binary collisions

We assume particles are of equal size and mass possessing no tangential component ($\mu = 0$ and $v_{t,0} = 0$). For a binary collision it follows that:

$$\bar{v}_n = \bar{v}_{n,0} - \frac{1+e}{2} \bar{v}_{ab,n} \quad (1)$$

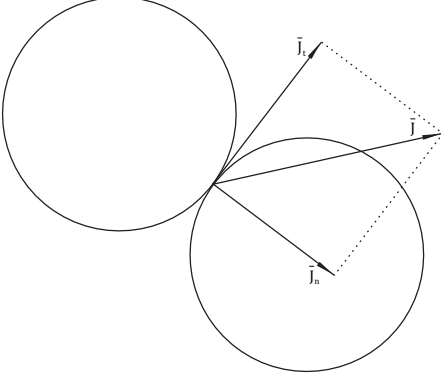
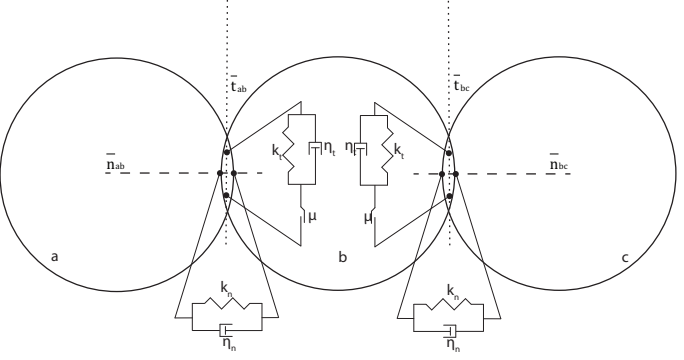
with \bar{v}_{ab} defined as the relative velocity at the point of contact:

$$\bar{v}_{ab} = \bar{v}_a - \bar{v}_b + (\bar{\omega}_a R_a + \bar{\omega}_b R_b) \times \bar{n}_{ab} \quad (2)$$

which consists of a normal and a tangential component:

$$\bar{v}_{ab,n} = (\bar{v}_{ab} \cdot \bar{n}_{ab}) \bar{n}_{ab} \quad (3)$$

Table 1: Short overview of the hybrid collisions schemes.

Hybrid model	
	
<p>Binary</p> $\bar{v}_{n,a} = \bar{v}_{n,a,0} - \frac{1+e}{2} \bar{v}_{ab,n}$ $\bar{x}_a = \bar{x}_{a,0} + \frac{\bar{v}_a + \bar{v}_b}{2} \Delta t + (\bar{v}_a - \bar{v}_{n,a,0}) t_{last}$ $t_{last} = \frac{(\bar{r}_{ab} \cdot \bar{v}_{ab} + \sqrt{(\bar{r}_{ab} \cdot \bar{v}_{ab})^2 - (\bar{r}_{ab} - (R_a + R_b))^2 \bar{v}_{ab} })}{ \bar{v}_{ab} }$	<p>Multibody</p> $\bar{F}_n = -k_n \delta_n \bar{n}_{ab} - \eta_n \bar{v}_{ab,n}$ $\bar{F}_t = -k_t \delta_t \bar{t}_{ab} - \eta_t \bar{v}_{ab,t}$ <p>or in case of sliding ($\bar{F}_t > \mu \bar{F}_n$):</p> $\bar{F}_t = -\mu \bar{F}_n \bar{t}_{ab}$
<p>Time scale collision</p> $t_{coll} = \frac{\pi}{\omega_d}$	<p>Time scale collision</p> $t_{coll} \leq \frac{\pi}{\omega_d}$
<p>Time step</p> $\Delta t = t_{coll}$	<p>Time step dilation in case of multibody</p> $\Delta t = \frac{t_{coll}}{10}$

$$\bar{v}_{ab,t} = \bar{v}_{ab} - \bar{v}_{ab,n} \quad (4)$$

$$\bar{n}_{ab} = \frac{\bar{x}_b - \bar{x}_a}{|\bar{x}_b - \bar{x}_a|} \quad (5)$$

$$\bar{t}_{ab} = \frac{\bar{v}_{ab,t}}{|\bar{v}_{ab,t}|} \quad (6)$$

Finally the position is defined as:

$$\bar{x} = \bar{x}_0 - \bar{v}_0 t_{last} + \frac{\bar{v}_a + \bar{v}_b}{2} \Delta t + \bar{v} t_{last} \quad (7)$$

That is, the new position is the sum of respectively the old position, the displacement until collision based on the old velocity, a shared mean displacement of the two particles during collision and a displacement after the collision till the end of the time step.

Here, \bar{x}_0 and \bar{v}_0 are the position and velocity at the time step before collision, and \bar{x} and \bar{v} the position and velocity at the time step after the collision. t_{last} is the time between the moment of first contact until the end of the time step. These are given by:

$$\bar{r}_{ab} = \bar{x}_{a,0} - \bar{x}_{b,0}$$

$$\bar{v}_{ab} = \bar{v}_{a,0} - \bar{v}_{b,0}$$

$$t_{last} = \frac{(\bar{r}_{ab} \cdot \bar{v}_{ab} + \sqrt{(\bar{r}_{ab} \cdot \bar{v}_{ab})^2 - (|\bar{r}_{ab}| - (R_a + R_b))^2 |\bar{v}_{ab}|})}{|\bar{v}_{ab}|} \quad (8)$$

Multi-body collisions

The analytical solution to multi-body contacts follows a very similar equation as those for binary collisions:

$$x_i(t) = \sum_{i=1}^n e^{-\zeta \omega_n t} (d_{1,i} \cos(\omega_{d,i} t) + d_{2,i} \sin(\omega_{d,i} t)) \quad (9)$$

where n is the number of contacts. Even though it is possible to determine trajectory and the change of velocity of the MBC, it is not possible to determine the duration of the collision analytically, as the sum of sinusoids with differing frequencies and amplitudes cannot be easily simplified. As such it is not possible to determine the outcome of a MBC in this particular way. On top of this because of the added amplitudes and frequencies the collision can take both longer and shorter than the original binary collision duration.

Keeping the above in mind it is simpler to use the classical soft sphere treatment, and divide the contact time into a number of steps only for the particles in an MBC, see also table 1.

Overview of DEM code

Here we will give a brief description of the code. The code is build using MATLAB for simple training purposes. To allow each binary collision to be uniquely described the time step is taken as exactly the duration of a collision following the soft-sphere approach, given by:

$$\Delta t = t_{coll} = \frac{\pi}{\omega_d} = \frac{\pi}{\sqrt{\frac{k_n}{m_{eff}} (\sqrt{1 - \zeta^2})}} \quad (10)$$

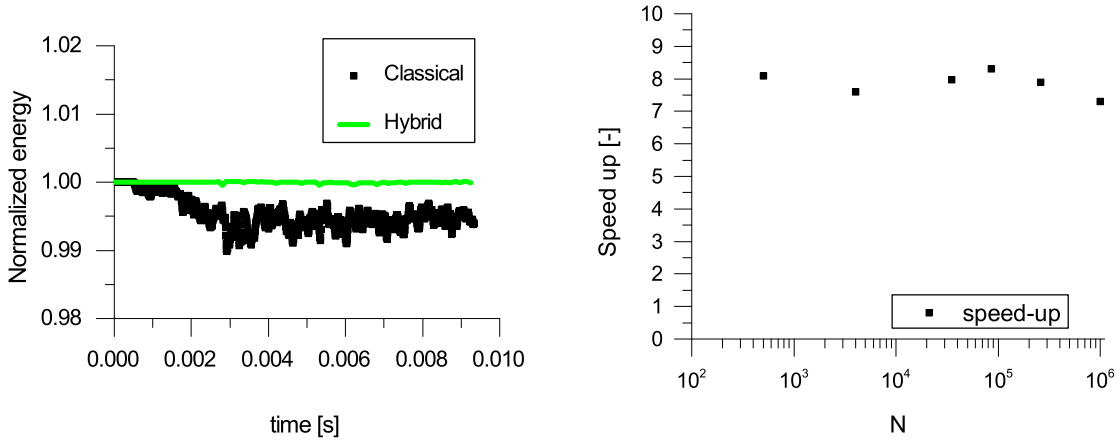


Figure 2: Normalized energy levels per time step for a bounding box problem with $e=1$. In black the classical soft-sphere method is given, in green the new hybrid model (left). Speed up as a function of the number of particles N (right).

where ω_d is the dampened frequency defined as:

$$\omega_d = \sqrt{\frac{k_n}{m_{eff}}} \left(\sqrt{1 - \zeta^2} \right)$$

where ζ is the damping ratio defined as:

$$\frac{-\ln(e)}{\sqrt{\pi^2 + \ln(e)^2}}$$

A collision detection algorithm; a kd-tree searcher, from MATLAB is used to detect all particles that have overlap. For these particles the duration of the contact is determined using equation 8 and subsequently the collision is processed with the method described earlier. For multi-body collisions the duration of a collision can be slightly longer or shorter as described before. In case the collision takes longer the information has to be appropriately transferred across time steps.

Additionally, checks have to be made for particles that are colliding in two subsequent time steps, because the two collisions might be overlapping, in essence being a multi-body collision. this has extensively been discussed in Buist *et al.* (2016).

RESULTS

Table 2: Parameter values used for the simulations.

parameter	value	
ϕ_s	0.4-0.5	
N_p	$10^3 - 10^6$	
d_p	0.003	m
ρ	2500	kg/m^3
k_n	20000	N/m
e	0.7-1.0	
β	1	
μ	0	
$\langle v_n \rangle$	0	m/s
v_t	0	m/s
v_{max}	± 0.15	m/s

In this section the first results of the new integration scheme will be shown. First tests are done for a bounding box problem. This problem consists of a cubic box randomly filled

with particles, with sizes ranging from 8 to 100 times the particle diameter. The particles have zero mean velocity and are given a velocity drawn from a Gaussian distribution. The maximum velocity, solids fraction and the box size can be varied to scale the problem. The simulation data is given in table 2 and are inspired by simulations of a fluidized bed (see figure 1), to match the solids holdup and granular temperature. For the particle-wall contacts we assume the same restitution coefficient as for particle-particle contacts.

Speed up & Scalability

The first test involves a bounding box containing 4000 particles with a solids volume fraction of 40%. The particles are allowed to freely bounce in the box for 0.1 s of real time. Simulations were conducted using both the new collision integration scheme as well as the classical soft sphere scheme. This resulted in on average 50 collisions per particle and 0.4 multibody collisions per particle. In this test the particles have ideal collision properties. This implies that the total energy in the system should remain constant. The normalized total kinetic energy of the particles is shown in figure 2. The total energy is normalized to the energy given at $t=0$.

The classical soft sphere method shows regular dips in the energy-level, associated with energy being stored in the springs as a consequence of the collisions. The hybrid model has a largely static energy profile as most collisions are binary. Both models are capable of maintaining proper energy conservation, as expected. The difference is however that the hybrid model is about eight times faster.

To test for the scalability of the hybrid model and the robustness of the gained speed up, the size of the bounding box is gradually increased to include 10^6 particles. The relative speed up for these systems is shown in figure 2. It can be seen that an average speed up of a factor 7 to 8 is possible with the new hybrid collision integration scheme. This speed up can be attributed to the lower number of collision detection evaluations that are necessary. The maximum possible speed-up factor 10 is not reached because of the overhead associated with the check for overlapping collisions, as discussed in the previous section.

Number of contact partners

For the new hybrid model to be competitive with the classical soft sphere model, it has to be capable of dealing with sys-

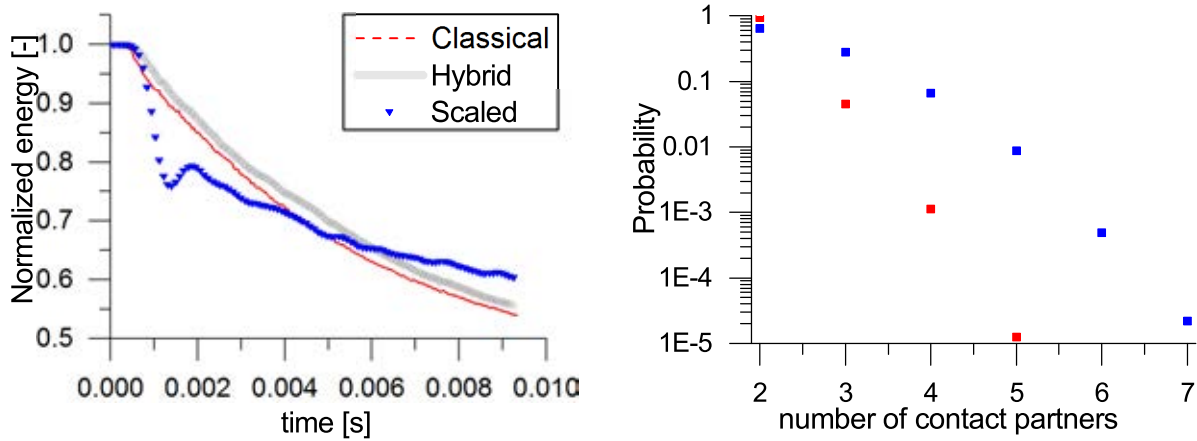


Figure 3: Normalized energy loss over time for the two schemes (left), collision order probability (right), for a bounding box problem with $\varepsilon = 0.5$, $e = 0.9$, $\mu = 0$.

tems with similar solids fractions and granular temperatures. It is the combination of these two parameters that determines the amount of multibody collisions. For this reason a simulation was run with a solids fraction of 50% and a maximum velocity of 0.15 m/s. The results are shown in figure 3. The left figure shows the normalized energy of the system for the two schemes, the figure on the right shows the probability of the number of contact partners, with 2 being binary and every higher number signifying extra particles participating in the collision. It can be seen that the two models show the same trend, now with more energy stored in the springs for the classic model. The amount of multibody collisions add up to about 5% of all collisions which matches the result of figure 3. The hybrid model is thus able to match the density and energy of systems in which typically a soft sphere model is used.

Relaxing the classical scheme

In the classical scheme it is also possible to scale the duration of a collision by scaling the spring stiffness. By reducing the spring stiffness by a factor 100, the duration of a collision is multiplied by a factor ten, i.e. the same as for our hybrid model. This will reduce computation time but will also increase the overlap between colliding particles.

To see if this affects the energy balance of the system, the results of such scaling of the spring stiffness is quantified for the same simulation as before, figure 3 in comparison to the classical and the hybrid schemes. The number of contact partners is also shown for the scaled model. The first thing that can be seen is that the scaled scheme has a very sudden and large drop in energy, associated with a lot of particles entering collision mode at the same time, often with multiple collision partners. Binary collisions only make up for 65 % of all collisions. The rate of energy loss is also much smaller than for the classical and the hybrid schemes.

This underestimation of the dissipation rate is entirely attributable to the number of multibody contacts and was also found for pure multibody contacts in Pournin *et al.* (2001). The relative speed up of the scaled model is only in the order of 2.5. The poor performance of this scaled classic model, in terms of both the energy conservation and the speed up of the model, shows the power and need of a hybrid model all the more. Second, the lower rate of energy dissipation means that the choice of a proper spring stiffness is critical in obtaining meaningful results, especially for dense dynamical

systems.

CONCLUSIONS

Most collisions in a soft-sphere granular flow problem are necessarily binary that can be accurately described within one time step. Because of the possible distinction between binary and multi-body contacts a hybrid collision integration scheme was proposed. The binary collisions are solved with a modified hard-sphere approach with a collision duration equal to the classic linear spring dashpot and all multi-body contacts are handled with the classic soft-sphere approach.

The larger time-step of this hybrid integration scheme and the lower amount of collision detection evaluations allows for a factor 7 to 8 computational speed-up. Meanwhile retaining energy and momentum conservation. Because a lower amount of energy is stored in the springs of the spring-dashpot model the energy state of the hybrid scheme more accurately describes the granular behaviour of the system.

The results of this scheme were shown to be scalable with the number of particles up to at least $O(10^6)$ and is capable of handling systems with a solids hold-up and granular temperature resembling the collision dynamics in an actual granular flow system.

Further relaxation of the spring-stiffness in the classical scheme to allow for a similar increase in time-step has proven to be inadequate to quantitatively capture the energy decay of a dense dynamic granular system and was proven to be less computationally efficient as the presented hybrid scheme.

ACKNOWLEDGEMENTS

This research was funded by the European Research Council, under the Advanced Investigator Grant Scheme, contract no. 247298 (Multiscale Flows).

REFERENCES

- BUIST, K.A., VAN ERDEWIJK, T.W., DEEN, N.G. and KUIPERS, J.A.M. (2015). "Determination and comparison of rotational velocity in a pseudo 2-d fluidized bed using magnetic particle tracking and discrete particle modeling". *AIChE Journal*, **61**(10), 3198–3207.
- BUIST, K.A., SEELEN, L., DEEN, N., PADDING, J. and KUIPERS, J. (2016). "On an efficient hybrid soft and hard sphere collision integration scheme for dem". *Chemical Engineering Science*, **153**, 363–373.
- CLEARY, P.W. and SAWLEY, M.L. (2002). "Dem modelling of industrial granular flows: 3d case studies and the

effect of particle shape on hopper discharge”. *Applied Mathematical Modelling*, **26(2)**, 89–111.

CUNDALL, P.A. and STRACK, O.D. (1979). “A discrete numerical model for granular assemblies”. *Geotechnique*, **29(1)**, 47–65.

DEEN, N.G., VAN SINT ANNALAND, M., VAN DER HOEF, M.A. and KUIPERS, J.A.M. (2007). “Review of discrete particle modeling of fluidized beds”. *Chemical Engineering Science*, **62(1)**, 28–44.

GONZALEZ BRIONES, J.S.L., WINDOWS-YULE, C.R., LUDING, S., PARKER, D.J. and THORNTON, A.R. (2015). “Shaping segregation: Convexity vs. concavity”. *Physical review B: Condensed matter*, 1–5.

GUI, N., YANG, X., JIANG, S., TU, J. and FAN, J. (2016). “Extended hpm–dem coupled simulation of drainage of square particles in a 2d hopper flow”. *AIChE Journal*.

HELLAND, E., OCCELLI, R. and TADRIST, L. (2002). “Computational study of fluctuating motions and cluster structures in gas–particle flows”. *International Journal of Multiphase Flow*, **28(2)**, 199–223.

HOOMANS, B.P.B., KUIPERS, J.A.M., BRIELS, W.J. and VAN SWAAIJ, W.P.M. (1996). “Discrete particle simulation of bubble and slug formation in a two-dimensional gas-fluidised bed: a hard-sphere approach”. *Chemical Engineering Science*, **51(1)**, 99–118.

KOREVAAR, M.W., PADDING, J.T., VAN DER HOEF, M.A. and KUIPERS, J.A.M. (2014). “Integrated dem–cfD modeling of the contact charging of pneumatically conveyed powders”. *Powder technology*, **258**, 144–156.

LU, G., THIRD, J.R. and MÜLLER, C.R. (2015). “Discrete element models for non-spherical particle systems: From theoretical developments to applications”. *Chemical Engineering Science*, **127**, 425–465.

MARSHALL, J.S. (2009). “Discrete-element modeling of particulate aerosol flows”. *Journal of Computational Physics*, **228(5)**, 1541–1561.

MIKAMI, T., KAMIYA, H. and HORIO, M. (1998). “Numerical simulation of cohesive powder behavior in a fluidized bed”. *Chemical Engineering Science*, **53(10)**, 1927–1940.

POURNIN, L., LIEBLING, T.M. and MOCELLIN, A. (2001). “Molecular-dynamics force models for better control of energy dissipation in numerical simulations of dense granular media”. *Physical Review E*, **65(1)**, 011302.

POURNIN, L., WEBER, M., TSUKAHARA, M., FERREZ, J.A., RAMAIOLI, M. and LIEBLING, T.M. (2005). “Three-dimensional distinct element simulation of spherocylinder crystallization”. *Granular Matter*, **7(2-3)**, 119–126.

SHIRSATH, S.S., PADDING, J.T., KUIPERS, J.A.M., PEETERS, T.W.J. and CLERCX, H.J.H. (2014). “Numerical investigation of monodisperse granular flow through an inclined rotating chute”. *AIChE journal*, **60(10)**, 3424–3441.

TSUJI, Y., KAWAGUCHI, T. and TANAKA, T. (1993). “Discrete particle simulation of two-dimensional fluidized bed”. *Powder technology*, **77(1)**, 79–87.

VAN BUIJTENEN, M.S., BÖRNER, M., DEEN, N.G., HEINRICH, S., ANTONYUK, S. and KUIPERS, J.A.M. (2011). “An experimental study of the effect of collision properties on spout fluidized bed dynamics”. *Powder Technology*, **206(1)**, 139–148.

XU, B.H. and YU, A.B. (1997). “Numerical simulation of the gas-solid flow in a fluidized bed by combining discrete particle method with computational fluid dynamics”. *Chemical Engineering Science*, **52(16)**, 2785–2809.

YANG, R.Y., YU, A.B., MCELROY, L. and BAO, J.

(2008). “Numerical simulation of particle dynamics in different flow regimes in a rotating drum”. *Powder Technology*, **188(2)**, 170–177.

ZASTAWNY, M., MALLOUPPAS, G., ZHAO, F. and VAN WACHEM, B. (2012). “Derivation of drag and lift force and torque coefficients for non-spherical particles in flows”. *International Journal of Multiphase Flow*, **39**, 227–239.

ZHU, H.P., ZHOU, Z.Y., YANG, R.Y. and YU, A.B. (2007). “Discrete particle simulation of particulate systems: theoretical developments”. *Chemical Engineering Science*, **62(13)**, 3378–3396.

ZHU, H.P., ZHOU, Z.Y., YANG, R.Y. and YU, A.B. (2008). “Discrete particle simulation of particulate systems: a review of major applications and findings”. *Chemical Engineering Science*, **63(23)**, 5728–5770.